第38卷第1期
2019年2月

红外与毫米波学报
J. Infrared Millim. Waves

Vol. 38, No. 1
February, 2019

文章编号: 1001-9014(2019)01-0008-07

DOI: 10.11972/j.issn.1001-9014.2019.01.002

Design method for triple conjugate optical system with good stray light control performance

YU Qing-Hua[1,2], XIAO Xi-Sheng[1,2,3], CHEN Fan-Sheng[1,2], SUN Sheng-Li[1,2*]

(1. Shanghai Institute of Technical Physics of the Chinese Academy of Sciences, Shanghai, 200083, China;
2. Key Laboratory of Intelligent Infrared Perception, Chinese Academy of Sciences, Shanghai, 200083, China;
3. University of Chinese Academy of Sciences, Beijing 100049, China)

Abstract: Stray light control is an important technical indicator of an optical system's performance. The stray light in infrared optical systems includes not only external stray light, but also the internal radiation stray light. The conventional initial system design method limited to an "object-image" conjugate relationship cannot properly take account of stray light. This paper presents a triple conjugate optical system design method for "object-image", "object-intermediate real image" and "entrance pupil-exit pupil" triple conjugate relationships that minimizes the influences of internal and external stray light to provide good stray light control performance. With this method, an off-axis three-mirror anastigmatic infrared optical system with F/# = 4, linear field of view = 7°, point source transmission less than 5×10^{-4}, and cold iris efficiency 96% was designed and imaged good pictures in orbit.

Key words: imaging systems, geometric optical design, infrared optical remote sensor
PACS: 07.57.Kp, 07.07.Df, 07.05.Tp

三重共轭消杂散光光学系统的设计方法研究

于清华[1,2], 肖锡晟[1,2,3], 陈凡胜[1,2], 孙胜利[1,2*]

(1. 中国科学院上海技术物理研究所, 上海 200083;
2. 中国科学院红外智能感知重点实验室, 上海 200083;
3. 中国科学院大学, 北京 100049)

摘要: 杂散光抑制能力是光学系统的重要评价指标. 红外光学系统不仅受到外部杂散光影响, 而且受到仪器内部杂散光影响. 传统的"物-像"共轭光学系统的设计方法未能全面考虑杂散光的抑制问题. 提出一种三重共轭光学系统的设计方法, 该方法设计出的光学系统具有"物-像"、"物-中间像"和"入瞳-出瞳"三重共轭关系, 具有同时抑制内部和外部杂散光的能力. 基于该方法设计出一种离轴三反射式消像散光学系统, 该系统 F/# = 4、一维线视场 7°, 离轴 5 度视场外点源透过率低于 5×10^{-4}, 系统冷屏效率达到 96%, 并获得良好的在轨图像.

关 键 词: 成像系统; 几何光学设计; 红外光学遥感仪器

中图分类号: O435.2 **文献标识码:** A

Introduction

Stray light, which is defined as any unwanted light arriving on the focal plane of an optical system, can degrade image contrast and image quality, and even completely submerge the target signal in the noise it causes [1-4]. Several Earth imaging systems have been affected by diffuse and coherent stray light to a significant degree [5]. SeaWiFS and MODIS experienced "unforeseen" ghosting that had to be corrected using in-orbit processing. Advanced Land Imager, the pathfinder for the Landsat-8/Operational Land Imager instrument, discovered ghosting levels of approximately 1% close to the

Received date: 2018-04-12, **revised date:** 2018-10-05 **收稿日期:** 2018-04-12, **修回日期:** 2018-10-05
Foundation items: Supported by Youth Innovation Promotion Association of the Chinese Academy of Sciences (20150192); The equipment department of the space system department (30508020216)
Biography: YU Qing-Hua (1981-), female, Hebei, PHD. Research area involves remote sensors and devices. E-mail: yuqinghua2000@126.com
* **Corresponding author:** E-mail: palm_sun@mail.sitp.ac.cn

?1994-2019 China Academic Journal Electronic Publishing House. All rights reserved. http://www.cnki.net

edge of the extended object for three of the bands [5]. Effective stray light control is thus a key requirement for wide dynamic range performance of scientific optical and infrared systems [6].

Stray light in visible optical systems is external stray light, such as the sunlight passing through the lens barrel to the focal plane. The stray light in infrared optical systems includes not only external stray light, but also the internal radiation stray light, which radiates from the instrument itself and reaches the focal plane [7-8]. Stray light control methods include baffles, diaphragms, vanes, and layers. Because the spectral emissivity is equal to the spectral absorptivity, control methods for the external and internal stray light in infrared optical systems are usually contradictory [2]. A preferred way to achieve a good balance in controlling external and internal stray lights is to provide a good optical structure with an intermediate real image plane and a real exit pupil in the optical path. By putting a field stop at the location of the intermediate real image, the optical system can be divided into two different parts. In the front part, the external stray light is controlled using baffles, vanes, and layers with high absorptivity. In the rear part, the internal stray light is controlled by placing a cold iris in the real exit pupil position. An optical system with such a configuration has three conjugate relationships: "object-image", "object-intermediate real image", and "entrance pupil-exit pupil".

However, the existing available initial system design method is solely applicable to systems with only the "object-image" conjugate relationship [9-10]. Although some optical systems with intermediate real images or real exit pupils are used, such as Korsch [11], there is still no method reported for designing the triple conjugate optical system described above.

Owing to the nature of optimization, a good starting point is usually very important in the design of an imaging system, especially in a complicated system [12-13]. In this paper, we provide an initial system design method for the triple conjugate optical system and demonstrate its efficacy by designing an off-axis three-mirror anastigmatic (TMA) optical system. In step one, primary aberration theory is used to describe the "object-image", "object-intermediate real image", and "entrance pupil-exit pupil" triple conjugate relationships in the coaxial optical system. In step two, three constraints are given: 1) intermediate real image position is in the optical path; 2) real exit pupil position is before the focal image plane; and 3) system F/# meets the target optical system F/# requirement. In step three, the initial optical structural parameters are solved using the numerical least squares method. In the final step, an optimization method is applied for structural conversion from coaxial system to off-axis system.

The remainder of this paper is organized as follows. In Section 2, the proposed design method for optical systems with three conjugate relationships is provided and described through the design of an off-axis TMA optical system. In Section 3, an infrared off-axis TMA optical system is designed to verify the provided design method, which has good performance in controlling internal and external stray light. An initial structure of an off-axis TMA infrared optical system is calculated according to Section 2, and then optimized through the optical software to obtain good image quality. Section 4 concludes this paper.

1　Design Method

The optical configuration with an intermediate real image and a real exit pupil can be very effective in controlling stray light. Such a configuration is depicted in Fig. 1. The optical system is divided into two different parts by a field stop placed at the intermediate real image plane. In the front part, the external stray light is controlled; in the rear part, a cold iris is placed at the real exit pupil to control the internal stray light. One intrinsic feature of this optical system is that it has a set of three conjugate relationships: "object-image", "object-intermediate real image", and "entrance pupil-exit pupil". We propose a design method on the basis of these conjugates.

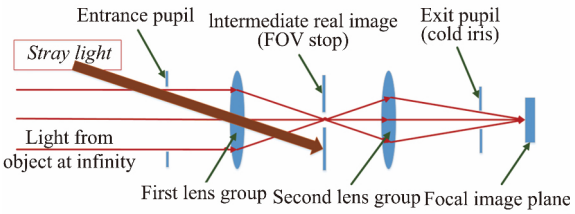

Fig. 1　Sketch map of optical system with good stray light control performance

图 1　具有较强杂散光抑制能力的光学结构图

The design method comprises the following steps.

Step one: primary aberration theory is used to describe the "object-image", "object-intermediate real image", and "entrance pupil-exit pupil" triple conjugate relationship in the coaxial optical system.

Step two: three constraints are given: 1) intermediate real image position is in the optical path; 2) real exit pupil position is before the focal image plane; and 3) system F/# meets the target optical system F/# requirement.

Step three: the initial optical structural parameters are solved using the numerical least squares method.

Off-axis TMA optical systems are widely used because of their various advantages, especially in infrared optical systems [4,10-11,14]. Therefore, in this paper, an initial system design method for a triple conjugate optical system is examined and described through the off-axis TMA optical system.

Aperture off-axis and field of view (FOV) off-axis optical systems can be considered to be the off-axis portions of coaxially optical systems [11,14]. The starting point for the off-axis TMA infrared optical system is the coaxial TMA optical system.

The coaxial TMA optical path with the "object-image", "object-intermediate real image", and "entrance pupil-exit pupil" triple conjugate relationship is shown in Fig. 2. The light from an object at infinity passes through the entrance pupil, primary mirror M_1, and secondary mirror M_2, focuses onto the intermediate real im-

?1994-2019 China Academic Journal Electronic Publishing House. All rights reserved.　http://www.cnki.net

age plane, and then passes the tertiary mirror M_3 and exit pupil, and focuses onto the focal image plane. The entrance pupil is an object with a limited distance in the TMA optical path. The light from the entrance pupil passes the TMA optical path and are focused onto the exit pupil.

The optical paths for "object-image", "object-intermediate real image", and "entrance pupil-exit pupil" triple conjugate relationship are shown in Figs. 3and 4 respectively. Those satisfy the paraxial aberration theory.

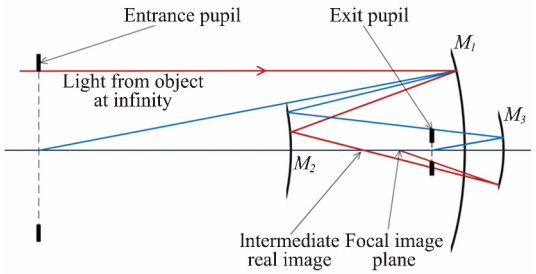

Fig. 2 TMA optical path for an object at infinity
图2 对无穷远目标成像的三反射式光学系统

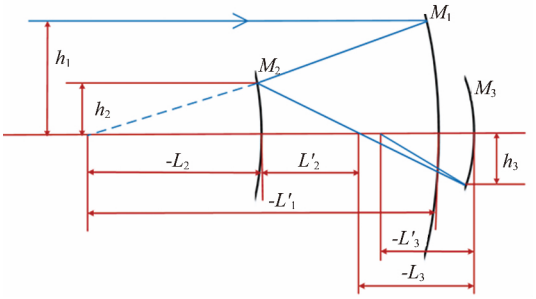

Fig. 3 Optical path for "object-image" and "object-intermediate real image" conjugate relationships
图3 "物-像"和"物-中间像"两重共轭光路

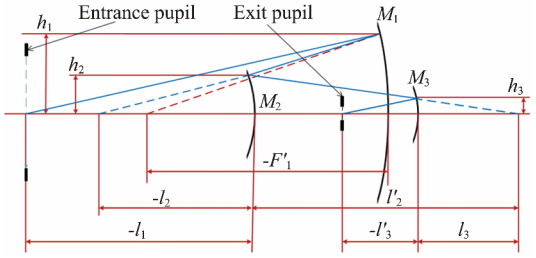

Fig. 4 Optical path for "entrance pupil-exit pupil" conjugate relationship
图4 "入瞳-出瞳"共轭光路

The first conjugate relationship of the TMA optical system, "object-image", is illustrated in Fig. 3. The object is at infinity. The object light is incident in the TMA optical system, reflected by the primary mirror M_1, secondary mirror M_2, and tertiary mirror M_3 in succession, and then focuses onto the image plane. The radius of the entrance pupil is normalized to one. The incident angle from the object at infinity is zero. According to the PW method of paraxial aberration theory, the PW parameters in the primary aberration formula are as follows [14]. The subscript numbers for P, W, h, and y consist of two digits; the first digit represents the first conjugate relationship, the second digit represents the number of the mirror.

$$P_{11} = \frac{1}{4}\left(\frac{L_2' \cdot L_3'}{L_2 \cdot L_3}\right)^3 , \quad (1)$$

$$P_{12} = -\frac{1}{4}\left(\frac{L_3'}{L_3}\right)^3\left(1+\frac{L_2'}{L_2}\right)\left(1-\frac{L_2'}{L_2}\right)^2 , \quad (2)$$

$$P_{13} = -\frac{1}{4}\left(1-\frac{L_3'}{L_3}\right)^3\left(1+\frac{L_3'}{L_3}\right)^2 , \quad (3)$$

$$W_{11} = \frac{1}{2}\left(\frac{L_2' \cdot L_3'}{L_2 \cdot L_3}\right)^2 , \quad (4)$$

$$W_{12} = -\frac{1}{2}\left(\frac{L_3'}{L_3}\right)^3\left(1-\frac{L_2'}{L_2}\right)\left(1+\frac{L_2'}{L_2}\right) , \quad (5)$$

$$W_{13} = -\frac{1}{2}\left(1+\frac{L_3'}{L_3}\right)^3\left(1-\frac{L_3'}{L_3}\right) , \quad (6)$$

$$h_{11} = 1 , \quad (7)$$

$$h_{12} = \frac{L_2}{F_1'} , \quad (8)$$

$$h_{13} = -\frac{L_3}{L_2'} \cdot \frac{L_2}{F_1'} , \quad (9)$$

$$y_{11} = 0 , \quad (10)$$

$$y_{12} = -\left(\frac{L_2}{F_1'}-1\right) \cdot \frac{L_2}{L_2'} \cdot \frac{L_3}{L_3'} , \quad (11)$$

$$y_{13} = \left[\frac{L_3}{L_2'}\left(\frac{L_2}{L_1'}-1\right)+\frac{L_2'}{L_2}\left(1+\frac{L_3}{L_2'}\right)\right] \cdot \frac{L_2}{L_2'} \cdot \frac{L_3}{L_3'} , \quad (12)$$

$$J = 1 . \quad (13)$$

F_1' is the focal length of the primary mirror on the image side; L_2 is the object's distance from the secondary mirror, the "object" is the image of the object at infinity imaged by the primary mirror; L_2' is the distance of the image from the secondary mirror; L_3 is the object's distance from the tertiary mirror, the "object" is the image of the object at infinity imaged by the primary and secondary mirrors; and L_3' is the distance of the image from the tertiary mirror.

The secondary conjugate relationship "object-intermediate real image" of the TMA optical system is also illustrated in Fig. 3. The object is at infinity. The object light is incident in the TMA optical system, reflected by primary mirror M_1 and secondary mirror M_2 in succession, and then focuses in the intermediate image plane after secondary mirror M_2. The pupil radius is normalized to one. The incident angle from the object at infinity is zero. The PW parameters in the primary aberration formula are as follows [14]. The subscript number for P, W, h, and y consist of two digits. The first digit represents the second conjugate relationship; the second digit represents the number of the mirror.

$$P_{21} = -\frac{1}{4}\left(\frac{L_2' \cdot L_3'}{L_2 \cdot L_3}\right)^3 , \quad (14)$$

?1994-2019 China Academic Journal Electronic Publishing House. All rights reserved. http://www.cnki.net

$$P_{22} = \frac{1}{4}\left(\frac{L_3'}{L_3}\right)^3\left(1+\frac{L_2'}{L_2}\right)\left(1-\frac{L_2'}{L_2}\right), \quad (15)$$

$$W_{21} = \frac{1}{2}\left(\frac{L_2' \cdot L_3'}{L_2 \cdot L_3}\right)^2, \quad (16)$$

$$W_{22} = \frac{1}{2}\left(\frac{L_3'}{L_3}\right)^2\left(1-\frac{L_2'}{L_2}\right)\left(1+\frac{L_2'}{L_2}\right), \quad (17)$$

$$h_{21} = 1, \quad (18)$$

$$h_{22} = \frac{L_2}{F_1'}, \quad (19)$$

$$y_{21} = 0, \quad (20)$$

$$y_{22} = \left(\frac{L_2}{F_1'}-1\right)\cdot\frac{L_2}{L_2'}\cdot\frac{L_3}{L_3'}, \quad (21)$$

$$J = 1. \quad (22)$$

The third conjugate relationship of the TMA optical system, "entrance pupil-exit pupil", is illustrated in Fig. 4. The object is the entrance pupil of the TMA optical system, which is finite in a limited position. The entrance pupil is imaged by the TMA optical system in the position of the exit pupil of the TMA optical system.

According to the triangular geometric relationships shown in Fig. 4, the incident light edge h_{3i} at the location of each mirror, the incident angle h_{3i} of each mirror, the exit angle h_{3i}' of each mirror, and the index of the reflective system n_{3i} and n_{3i}' satisfy Eqs. (23)-(34). The subscript numbers for u, n, and h consist of two digits. The first digit represents the third conjugate relationship; the second digit represents the number of the mirror.

$$OP_1 = -F_1' + L_2, \quad (23)$$

$$h_{31} = 1, \quad (24)$$

$$h_{32} = -l_2/(-l_2 + OP_1), \quad (25)$$

$$h_{33} = h_2 \cdot l_3/l_2', \quad (26)$$

$$u_{31} = 1/(-l_1 + OP_1), \quad (27)$$

$$u_{31}' = 1/(-l_2 + OP_1), \quad (28)$$

$$u_{32} = u_1', \quad (29)$$

$$u_{32}' = h_2/l_2', \quad (30)$$

$$u_{33} = u_2', \quad (31)$$

$$u_{33}' = -h_3/l_3', \quad (32)$$

$$n_{31} = n_{32}' = n_{33}' = 1, \quad (33)$$

$$n_{31}' = n_{32} = n_{33} = -1. \quad (34)$$

OP_1 is the distance between M_1 and M_2. l_1 is the distance between the finite object and the secondary mirror; l_2 is the distance of the object from the secondary mirror, the "object" is the image of the finite object imaged by the primary mirror; l_2' is the distance of the image from the secondary mirror; l_3 is the object's distance from the tertiary mirror, the "object" is the image of the finite object imaged by the primary and secondary mirrors; and l_3' is the distance of the image from the tertiary mirror. By substituting Eqs. (23)-(34) into Eqs. (35) and (36) [14], the PW parameters for the third conjugate relationship can now be solved:

$$P_{3i} = \left(\frac{u_i' - u_i}{1/(n_i') - 1/n_i}\right)^2 \cdot \left(\frac{u_i'}{n_i'} - \frac{u_i}{n_i}\right), \quad (35)$$

$$W_{3i} = \left(\frac{u_i' - u_i}{1/(n_i') - 1/n_i}\right) \cdot \left(\frac{u_i'}{n_i'} - \frac{u_i}{n_i}\right). \quad (36)$$

The PW parameters in the primary aberration formula are as follows. y_{3i} and J are obtained using (10), (11), (12), and (13) [14]. The subscript numbers for P, W, h, and y consist of two digits. The first digit represents the third conjugate relationship; the second digit represents the number of the mirror.

$$P_{31} = \frac{1}{4}\left(\frac{1}{F_1' - L_2 + l_1} - \frac{1}{F_1' - L_2 + l_2}\right)^2 \cdot \left(\frac{1}{F_1' - L_2 + l_1} + \frac{1}{F_1' - L_2 + l_2}\right), \quad (37)$$

$$P_{32} = -\frac{1}{4}\left(\frac{1}{F_1' - L_2 + l_2}\right)^3 \cdot \left(1-\frac{l_2}{l_2}\right) \cdot \left(1+\frac{l_2}{l_2}\right)^2, \quad (38)$$

$$P_{33} = -\frac{1}{4}\left(\frac{l_2}{l_2'}\frac{1}{F_1' - L_2 + l_2}\right)^3 \cdot \left(1-\frac{l_3}{l_3}\right) \cdot \left(1+\frac{l_3}{l_3}\right)^2, \quad (39)$$

$$W_{31} = -\frac{1}{2}\left(\frac{1}{F_1' - L_2 + l_1} - \frac{1}{F_1' - L_2 + l_2}\right) \cdot \left(\frac{1}{F_1' - L_2 + l_1} + \frac{1}{F_1' - L_2 + l_2}\right), \quad (40)$$

$$W_{32} = -\frac{1}{2}\left(\frac{1}{F_1' - L_2 + l_2}\right)^2 \cdot \left(1-\frac{l_2}{l_2}\right)\left(1+\frac{l_2}{l_2}\right), \quad (41)$$

$$W_{33} = -\frac{1}{2}\left(\frac{l_2'}{l_2}\frac{1}{F_1' - L_2 + l_2}\right)^2 \cdot \left(1-\frac{l_3'}{l_3}\right)\left(1+\frac{l_3'}{l_3}\right), \quad (42)$$

$$h_{31} = 1, \quad (43)$$

$$h_{32} = \frac{l_2}{F_1' - L_2 + l_2}, \quad (44)$$

$$h_{33} = \frac{l_3}{l_2'}\frac{l_2}{F_1' - L_2 + l_2}, \quad (45)$$

$$y_{31} = 0, \quad (46)$$

$$y_{32} = \left(\frac{l_2}{F_1'}-1\right)\cdot\frac{l_2}{l_2'}\cdot\frac{l_3}{l_3'}, \quad (47)$$

$$y_{33} = \left[\frac{l_3}{l_2'}\left(\frac{l_2}{F_1'}-1\right) - \frac{l_2'}{l_2}\left(1-\frac{l_3}{l_2}\right)\right]\cdot\frac{l_2}{l_2'}\cdot\frac{l_3}{l_3'}, \quad (48)$$

$$J = 1. \quad (49)$$

In addition, to constrain the positions of the intermediate real image plane and the exit real pupil, the following three constraints have to be satisfied:

Constraint 1: $h_{12} > 0$ and $h_{13} < 0$;

Constraint 2: $-l_3' < -L_3'$;

Constraint 3: F/# = $|(L_3'/(2h_{13})|$ is close to working F/#.

Constraint 1 specifies that there is an intermediate real image between the secondary mirror and the tertiary mirror. Constraint 2 specifies that there is a real exit pupil between the tertiary mirror and the focal image plane.

The relative parameters F_1', L_2, L_2', L_3, L_3', l_2, l_2', l_3, and l_3' define the initial structure of the optical system directly; therefore, solving them is a key step. The number of relative parameters is nine; therefore, in addition to the three constraints above, another six equations are needed to solve these relative parameters. Three conjugate relationships described by Eqs. (1) ~ (22) and Eqs. (37) ~ (49) are brought into the PW method of the primary spherical aberration and primary coma ab-

?1994-2019 China Academic Journal Electronic Publishing House. All rights reserved. http://www.cnki.net

erration, and all made equal to zero to get six equations. Primary spherical aberration: $\sum S_{\mathrm{I}} = \sum hP$; primary coma aberration: $\sum S_{\mathrm{II}} = \sum yP - J\sum W$. Using the above six equations and three constraints, nine relative parameters in the initial structure of the paraxial optics can be solved using the multi-objective calculation method. Furthermore, according to the Gaussian optics and geometric relations described by the following equations, the vertex radius R_i of the three mirrors in the paraxial TMA optical system and the distances OP_i between mirrors are solved, which are initial structural parameters of the paraxial TMA optical system.

$$F_1' = R_1/2 \quad , \quad (50)$$

$$2/R_2 = 1/(-L_2') - 1/L_2 \quad , \quad (51)$$

$$2/R_3 = -1/L_3 - 1/(-L_3') \quad , \quad (52)$$

$$OP_1 = -F_1' + L_2 \quad , \quad (53)$$

$$OP_2 = L_2' + L_3 \quad , \quad (54)$$

$$OP_3 = -L_3' \quad . \quad (55)$$

The calculation of the initial structure of the coaxial TMA optical system with an intermediate real image plane and real exit pupil is completed using the above equations. Next, the initial structural parameters of the coaxial optical system are incorporated into the optical design software. Only the aperture and FOV of interest are optimized and evaluated, and the ideal parameters of the off-axis optical system with three conjugate relationships can be obtained [14-17].

2 Application Example

In this section, a design example is given to describe and demonstrate the design method. The specifications of the off-axis TMA infrared optical system are listed in Table 1. The point source transmittance (PST), which is defined as the ratio of the amount of stray light on the focal plane of an optical system to the amount of light incident at the entrance aperture of the system, is used to evaluate the ability to control external stray light.

Table 1 Specifications of off-axis TMA infrared optical system

表1 离轴三反红外光学系统的设计需求

Parameter	Specification
entrance pupil diameter	100 mm
F/#	4
linear FOV	7°
wavelength	2.1 μm to 4.8 μm
PST	less than 5×10^4 with off-axis angle > 5°
cold iris	efficiency > 95%

The off-axis TMA optical system can be considered as the off-axis portion of a coaxial optical system, as shown in Fig. 5. The aperture of the unshielded off-axis optical system was 100 mm, and the total axial diameter of the coaxial parent system was approximately 400 mm. The focal length was constant; thus, F/# of the coaxial parent system was approximately equal to 1.

According to the design method proposed in Section 2 for the off-axis TMA optical system, another additional

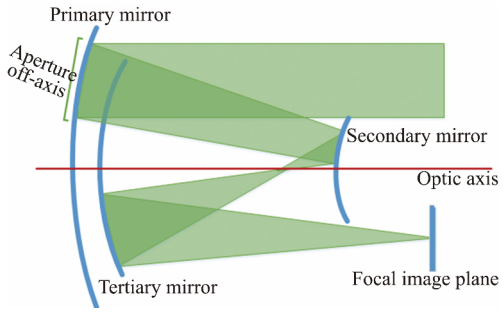

Fig. 5 Off-axis TMA optical system is the off-axis portion of the coaxial optical system

图5 离轴三反光学系统是同轴光学系统的离轴部分

constraint, "distance between primary and secondary mirror approximately equal to the distance between secondary mirror and tertiary mirror", needs to be satisfied. Nine relative parameters for the initial structure of the paraxial TMA optical system with triple conjugate relationships were calculated using minimum error value solving function fminsearch() in Matlab, as shown in Table 2.

Table 2 Relative Parameters of the Paraxial Optical System

表2 旁轴光学系统相关结构参数

Parameter	Value
F_1'	-1.480
L_2	-0.080
L_2'	0.069
L_3	-1.371
L_3'	-1.417
l_2	-2.632
l_2'	0.405
l_3	0.435
l_3'	-1.120

Equations (50) ~ (55) were used to calculate the initial structural parameters of the paraxial TMA optical system. The results are shown in Table 3.

Table 3 Initial Structural Parameters of the Paraxial Optical System

表3 旁轴光学系统初始结构参数

Parameter	Value
R_1	-2.961
R_2	-0.957
R_3	-1.420
OP_1	1.400
OP_2	1.440
OP_3	1.417

The effective aperture of the coaxial parent system was 400 mm. The initial structural parameters were no longer normalized and were therefore scaled by a radius of aperture 200 mm, as shown in Table 4. The wavefront error of the initial optical system was approximately 101λ, and the RMS spot radius was 3.2 mm.

Referring to the aperture or FOV of the off-axis optimization methods, the final structural parameters of the

?1994-2019 China Academic Journal Electronic Publishing House. All rights reserved. http://www.cnki.net

Table 4　Initial Structural Parameters of the Optical System
表 4　光学系统初始结构参数

Parameter	Value
R_1	−592.120 mm
R_2	−191.310 mm
R_3	−284.014 mm
OP_1	280.000 mm
OP_2	288.020 mm
OP_3	283.404 mm

triple conjugate optical system with good performance were optimized using an optical design program. The final structural parameters are shown in Table 5.

Table 5　Final Structural Parameters of the Optical System
表 5　光学系统最终结构参数

Parameter	Value
R_1 /conic	−600.1 mm/ −0.712 1
R_2 /conic	−186.092 mm/ −5.224
R_3 /conic	−266.701 mm/ −0.107 3
OP_1	280.000 mm
OP_2	288.020 mm
OP_3	271.182 mm

The final optimized optical system is shown in Fig. 6. The intermediate real image plane is between the secondary and tertiary mirrors, and the real exit pupil is between the tertiary mirror and the focal image plane.

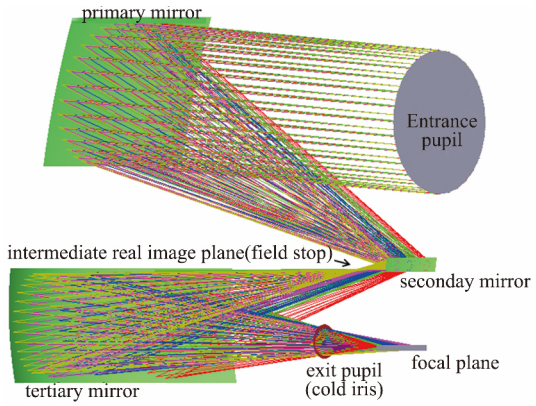

Fig. 6　Optical path
图 6　光路图

The F/# of the optical system is 4 and the linear FOV is 7°. The imaging quality of the optical system is close to the diffraction limit. The energy encircled in one pixel with a size of 28 μm is better than 75%, MTF is higher than 0.62 at 17.8 cy/mm, and wavefront error is 0.014 3λ, as shown in Figs. 7 ~ 9.

PST and cold iris efficiency are two important indicators for evaluating the ability of an optical system to control stray light. The ability to control stray light by the off-axis TMA infrared optical system was calculated and optimized in this paper is as follows:

1) The intermediate real image plane was approximately 26 mm behind the secondary mirror, where a field stop with rectangular aperture 54 mm × 6 mm was placed. It separated the optical path of the optical system into two relatively isolated parts. In the front part, the structures used highly absorptive layers inside, effectively controlling external stray light. The PST at an angle larger than 5° off-axis was lower than 5×10^{-4}, which is simulated and shown in Fig. 10.

2) The exit pupil distance was approximately 66 mm before the focal image plane, where the cold iris with aperture diameter 18.2 mm was placed and cooled to 150 K. The aperture of the cold iris was slightly smaller than the diameter of the footprint of the ray on the plane of the

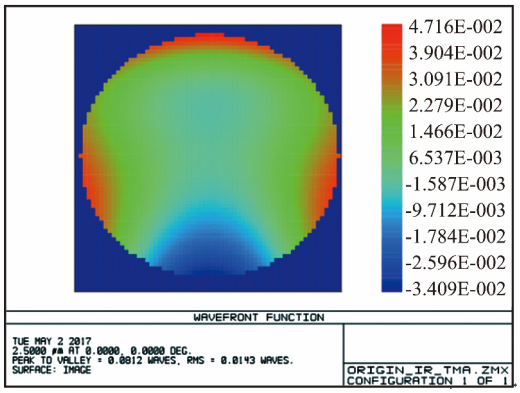

Fig. 7　Wavefront error map of the optical system
图 7　光学系统波前图

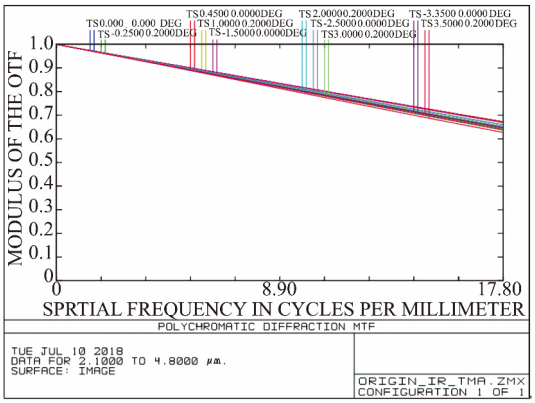

Fig. 8　MTF at frequency 17.8 cy/mm
图 8　在 17.8 cy/mm 处的 MTF

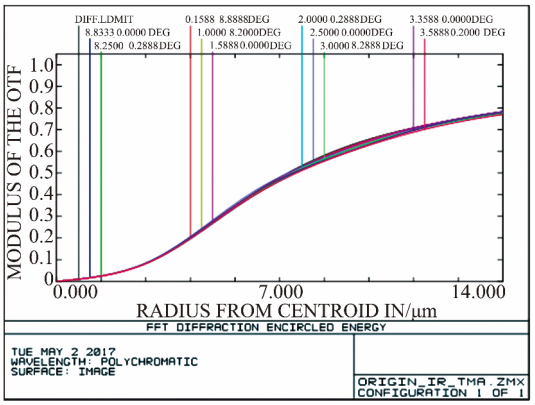

Fig. 9　Encircled energy by pixel with a size of 28 μm
图 9　像元尺寸 28 μm 内的能量集中度

?1994-2019 China Academic Journal Electronic Publishing House. All rights reserved.　http://www.cnki.net

exit pupil, such that the focal image plane through the cold iris can only see the tertiary mirror. The efficiency of the cold iris of the whole FOV was 96%, effectively controlling internal stray light.

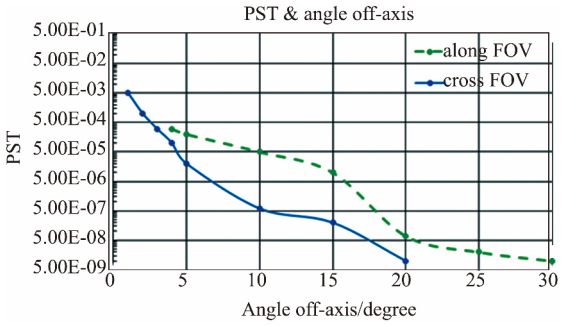

Fig. 10 PST varying with angle off-axis
图10 随离轴角变化的PST

This system had been used as a scanning remote sensor and imaged a lot of clear pictures in orbit. An example image is shown in Fig. 11, in which the water boundaries are clearly defined, and the dynamic range is about 1128:1.

Fig. 11 Picture achieved in orbit
图11 在轨拍摄的图片

3 Conclusion

In this paper, an initial system design method for a triple conjugate relationship optical system with good internal and external stray light control performance was proposed. Six equations were presented to describe the triple conjugate relationship comprising "object-image", "object-intermediate real image", and "entrance pupil-exit pupil". Three constraints were also presented to constrain the positions of the field stop and aperture diaphragms. These six equations and three constraints were used to solve for the nine relative parameters of the initial structure of the optical system.

To demonstrate the efficacy of the proposed design method, an off-axis TMA infrared optical system was calculated and optimized. The design achieved a wavefront error of 0.014 3λ, and PST at an angle larger than 5° off-axis that was lower than 5×10^{-4}. Further, the efficiency of the cold iris of the whole FOV was 96%. The results indicate that this infrared optical system can very effectively control external and internal stray lights.

Acknowledgments

This study was funded by the Youth Innovation Promotion Association of the Chinese Academy of Sciences (20150192) and the equipment department of the space system department (30508020216).

References

[1] Fest E. C. *Stray Light Analysis and Control* [M]. Bellingham: SPIE Press, 2013, 1-33.
[2] Montanaro M, Gerace A, Rohrbach S. Toward an operational stray light correction for the Landsat 8 Thermal Infrared Sensor [J]. *Appl. Opt.* 2015, **54**: 3963-3978.
[3] Yang J, Zhang R. Yin, L. *et al*. Study on a wideband, variable aperture, high resolution scatter meter for planar diffraction grating stray light measurement [J]. *Appl. Opt.* 2017, **56**: 247-255.
[4] Wang Q, Cheng D, Hou Q, *et al*. Stray light and tolerance analysis of an ultrathin waveguide display [J]. *Appl. Opt.* 2015, **54**: 8354-8362.
[5] Dabney P. W, Levy R, Ong L, *et al*. Ghosting and stray-light performance assessment of the Landsat data continuity mission's (LDCM) operational land imager (OLI) [J]. *Proc. SPIE*, 2013, 8866: 88661E.
[6] Patrick Waddell, Eric E. Becklin, Ryan T. Hamilton, *et al*. Telescope stray light: early experience with SOFIA [C]. *Proc. SPIE*, Infrared Remote Sensing and Instrumentation XXIV, 2016, 99730O.
[7] Tian Q, Chang S. Internal stray radiation measurement for cryogenic infrared imaging systems using a spherical mirror [J]. *Appl. Opt.* 2017, **56**: 4918-4925.
[8] Niu J, Shi S. Analysis to stray radiation of infrared detecting system [C]. *Proc. SPIE* 8193, International Symposium on Photoelectronic Detection and Imaging 2011: Advances in Infrared Imaging and Applications, 2011, 81931H.
[9] Zeng F, Zhang X. Zhang, J, *et al*. Optics ellipticity performance of an unobscured off-axis space telescope [J]. *Opt. Express*, 2014, **22**: 25277-25282.
[10] Tong Y, Jun Z. Guo, J. fan. Compact freeform off-axis three-mirror imaging system based on the integration of primary and tertiary mirrors on one single surface [J]. *Chinese Optics Letters*, 2016, **16**: 060801.
[11] Nie Y. Gross, H. Freeform optical design for a nonscanning corneal imaging system with a convexly curved image [J]. *Appl. Opt.* 2017, **56**: 5630-5638.
[12] Yang T, Zhu J, Hou, W, *et al*. Design method of freeform off-axis reflective imaging systems with a direct construction process [J]. *Opt. Express*, 2014, **22**: 9193-9199.
[13] Zhong Y, , Gross H. Initial system design method for nonrotationally symmetric systems based on Gaussian brackets and Nodal aberration theory [J]. *Opt. Express*, 2017, **25**: 10016-10030.
[14] Pan J. *Optical Aspheric Design, Processing and Testing* [M]. Beijing: *Science Press*, (潘君骅,光学非球面的设计、加工与检验,北京,科学出版社, 1994,10: 154.
[15] Tatian B. A first look at the computer design of optical systems without any symmetry [C]. *Proc. SPIE*, 1987, **766**: 38-47.
[16] Johnson R. B. Wide field of view three-mirror telescopes having a common optical axis [J]. *Opt. Eng.* **27**: 1046-1050 (1988).
[17] Pasquale B, Content D. Kruk, J. *et al*. Optical design of WFIRST-AFTA wide-field instrument [J]. *Classical Optics*, 2014, IM3A.7.

?1994-2019 China Academic Journal Electronic Publishing House. All rights reserved. http://www.cnki.net